*IN ·34
067087*

Numerical Simulation of a Low Emissions Gas Turbine Combustor Using KIVA-II

Part II: Quick-Quench/Lean-Combustion Zones Analysis

S.L. Yang and R. Chen
Michigan Technological University
Houghton, Michigan

M.C. Cline
Los Alamos National Laboratory
Los Alamos, New Mexico

August 1997

National Aeronautics and
Space Administration

NUMERICAL SIMULATION OF A LOW EMISSIONS GAS TURBINE COMBUSTOR USING KIVA-II, PART II: QUICK-QUENCH/LEAN-COMBUSTION ZONES ANALYSIS

S.L Yang* and R. Chen[†]
ME-EM Department
Michigan Technological University
Houghton, Michigan 49931

M.C. Cline
Los Alamos National Laboratory
Los Alamos, New Mexico

SUMMARY

This is the second part of the numerical investigation on a low emissions staged turbine combustor (STC) using a modified version of the KIVA-II code. The main focus of this study is the numerical analysis of the reacting fluid flow and heat transfer inside the quick-quench/lean-combustion (QQ/LC) zones. In the QQ zone, cool dilution air was injected into the hot mixture through eight 45° inclined slots with a momentum flux ratio of 60. The slot aspect ratio was 6 and the jet-to-mainstream mass flow rate ratio was 3. The inlet conditions of the QQ zone were obtained from the results of rich combustion zone analysis described in part I. A tension spline interpolation scheme was then used to interpolate the necessary information needed at the inlet. Conditions at the slot opening (dilution jet) were chosen closely related to those encountered in advanced combustion systems. The Grid system needed for the numerical solutions was generated by a transfinite interpolation scheme. KIVA-II was further modified for the current study.

Preliminary results illustrate some of the major features of the flow and temperature fields inside the QQ/LC zones. Formation of the co- and counter-rotating bulk flow and the sandwiched-ring-shape temperature field, typical of the confined inclined jet-in-cross flow, can be seen clearly and is consistent with experimental observations. The calculations of the mass-weighted standard deviation and the pattern factor of temperature revealed that the mixing performance of the STC combustor is very promising. The temperature of the fluid leaving the LC zone is very uniform. Prediction of the NOx emission index showed that there was no excessive thermal NOx produced in the QQ/LC zones for the case studied. From the results obtained so far, it appears that the modified KIVA-II code can be used to guide the low emission combustion experiments.

INTRODUCTION

This study is the second part of two part numerical investigation on a low emissions staged turbine combustor (STC) shown in figure 1. This STC combustor consists of a fuel nozzle (FN), a rich-burn (RB) zone, a converging connecting section, a quick-quench (QQ) zone, a diverging connecting section, and a lean-combustion (LC) zone. From the computational efficiency viewpoint, the STC combustor was divided into two subsystems, called the FN/RB zone and QQ/LC zones, and the numerical solutions were obtained separately for each subsystem with a considerable amount of zone overlap to minimize the effect of interzone boundary conditions. Part I (ref. 1) was concerned with the numerical study of the turbulent two-phase reacting flows inside the FN/RB zone using a modified version of the KIVA-II code (ref. 2). An advanced airblast fuel nozzle, which has two fuel injection passages and four air flow passages, was used for supplying air and fuel for the RB zone. Preliminary results were obtained and showed some of the major features of the flow and temperature fields inside the RB zone.

Numerical simulation of gas turbine combustors has become increasingly more important in the past decade. Solutions obtained by numerical method are often used to assist experimental studies which, in turn, will save time and money by reducing the number of tests and possible hardware modifications. However, complete numerical

---

*Associate Professor, to whom correspondence should be addressed.
[†]Graduate Research Assistant.

studies of potential complex STC combustors are still in their infancy. The most recent studies dealing with the QQ zone dilution jet mixing problems in flametube combustors can be found in references 3 to 7.[1] In their approach, the fluid and thermodynamic properties at the inlet of the QQ zone were assumed to be uniform and were estimated by a one-dimensional model for the RB zone. Their main focus was on the dilution jet mixing inside the QQ zone. Parameters, such as the momentum flux ratio, slot aspect ratio, and mixing flow area were investigated.

This paper describes the numerical analysis of the three-dimensional reacting fluid flow and heat transfer inside the QQ/LC zones. In these zones, cool dilution air was injected into the QQ section through inclined slots. A converging section was used to connect the RB and QQ zones and a diverging section was used to link the QQ and LC zones. The diameters of RB, QQ, and LC zones were in the ratio of 1.2 to 1.0 to 1.4. Inlet conditions of the QQ/LC zones were not assumed but were obtained from the rich combustion zone results as described in part I. Conditions at the slot opening (dilution jet) were chosen closely related to those encountered in advanced combustions systems.

DESCRIPTION OF PROBLEM

The system under investigation is the QQ/LC zones shown figure 1. To minimize the effect of the interzone boundary conditions, the inlet boundary was extended 1.8159 in. upstream of the convergence section. This location corresponds to one gridline in the RB zone (ref. 1). To avoid flow contamination due to the numerical outflow boundary conditions, the LB zone had a length of 6.3 in., i.e., 6.3 in. downstream of the divergence section. Figure 2 shows the geometry used to model the QQ/LC zones. In this figure, D and L_{quick} are the diameter and the length of the QQ zone, respectively.

There were eight equally spaced 45° inclined slots located around the perimeter of the QQ zone. The center of the slots was located at D/3 from the inlet of the QQ zone. The slot aspect ratio (length to width) was 6. Due to geometric symmetry, only one slot was modeled resulting in a 45° sector and the slot was symmetrically located at the center plane of the sector.

At the upstream inflow boundary, the hot rich mixture from the RB zone enters the QQ section. A tension spline interpolation (refs. 8 and 9) was then used to interpolate the necessary information at the inlet. The actual boundary conditions were the specification of the three velocity components, density, turbulent kinetic energy, and the turbulent length scale. Because the flow is subsonic, the pressure and temperature cannot be specified, but instead must be calculated as part of the solution. If the calculated pressure does not differ significantly from the RB zone value at the same location then the solution is assumed to be complete. However, if the calculated pressure differs significantly then the RB zone solution must be repeated. The new outflow boundary condition for the RB zone would be the pressure obtained from the QQ zone solution. This process would be repeated as necessary.

At the jet inflow boundary, the dilution jet was air (consisting of 76.8 percent N_2 and 23.2 percent of O_2) and entered the inclined slot with uniform radial velocity. The following jet inlet conditions were chosen in this study:

Temperature = 1000 °F (811 K)
Pressure = 90 psia (6.205×10^6 dynes/cm^2)
Jet-to-mainstream momentum flux ratio ($J = \rho_j V_j^2 / \rho_\infty V_\infty^2$) = 60
Turbulent kinetic energy = 0.1 of V_j
Turbulent length scale = 0.13 of D

where V_j and ρ_j are the jet inflow radial mean speed and density, respectively, and the subscript ∞ refers to the mainstream flow condition. The slot flow area was modified to maintain a constant jet-to-mainstream mass flow rate ratio (MJMR) of 3 and a slot orifice discharge coefficient of 0.6. The jet inlet boundary conditions were the specification of ρ_j (calculated form the temperature and pressure given above) and V_j (calculated from the J and MJMR given above). The turbulent intensity (v') and length scale were specified at the values given above, according to Talpallikar et al. (refs. 3 and 4). The exit boundary condition was to specify the pressure. The combustor walls were assumed to be adiabatic with a turbulent boundary layer. These conditions were enforced using wall functions (ref. 2). At the transverse boundaries (see fig. 2), periodic boundary conditions were applied.

---

[1]Reference 6 included the RB zone (premixed, prevaporized) and therefore the swirl entering the QQ zone was not assumed.

NUMERICAL METHOD OF SOLUTION

Since jet-in-cross flow is three-dimensional (3D), the dilution jet flow field was modeled as a 3D, compressible, and turbulent reacting flow and was closed by a κ–ε turbulent model with wall function. The numerical solutions were obtained by a modified version of KIVA-II, implemented to study the aforementioned objective.

Grid System

In order to generate a grid system for gas turbine combustor with inclined slots, an algebraic grid generation method has been developed (ref. 10) based on the transfinite interpolation (TI) method (refs. 11 and 12). As the details of this method can be found in reference 10, only the essence will be presented here.

To facilitate the grid generation scheme, the computational domain shown in figure 2 was divided into three subdomains: the RB zone together with the convergence section, the QQ zone, and the divergence section along with the LC zone. The TI method was first carried out for the QQ zone with grid lines passing exactly through the desired slot (size and location) with zero inclination angle. The next step was to use the TI method again for the other two subdomains but the grids were generated only for one axial-radial (z-r) plane. The final step was to patch the lines in the azimuthal (θ) direction based on the previously generated QQ zone 3D grid. A perspective view of the finished grids up-to-this-step is shown in figure 3. Figure 4 shows the cross-sectional views, r-θ plane and z-r plane, of figure 3. There were 51 points in the z direction, 21 points in the r direction, and 19 points in the θ direction.

To obtain the inclined slot grids, the mesh generated above was twisted by the desired angle about the center-line and a reference base plane (r-θ plane). Figure 5 shows the perspective view of the grid system with a 45° inclined slot in which the reference base plane was the inlet of the QQ zone (i.e. the last plane of the convergence section).

To see the effect of the twisted mesh on the solutions, a pure pipe flow with uniform inlet and without swirl was run for the grid system with and without twisting. As it was found that the fictitious swirl due to the twisted mesh was less than 1 percent and, thus, was considered insignificant. The grid system of figure 5 was used in this study.

Code Modifications

In addition to the modifications made to the basic KIVA-II code for the study of the FN/RB zone described in part I (ref. 1), further modifications are needed for current problem. Following are the descriptions of the additional changes made to the code.

The grid system, described above, was generated separately, and the KIVA-II code was modified to read the grid information accordingly in the input data routine. The geometry routines were modified so that the dilution slot on the right wall (from KIVA-II view) can be identified. The boundary condition routines were modified so that the inflow information at the slot can be specified. The data input routine was also modified to read the inlet boundary information obtained from the RB zone. Species information of air at the slot were also included.

To see the mixing effectiveness, the mass-weighted standard deviation (MWSD) and the pattern factor (PF) of temperature were selected and were included in the KIVA-II calculations. The MWSD and PF were defined as:

$$MWSD = \frac{\sqrt{\dfrac{\sum\limits_i m_i \left(T_i - T_{avg}\right)^2}{\sum\limits_i m_i}}}{T_{avg}} \tag{1}$$

$$PF = \frac{T_{max} - T_{avg}}{T_{avg} - T_{jet}} \qquad (2)$$

according to reference 3. The lower the value of MWSD and PF, the better the mixing that can be achieved.

RESULTS AND DISCUSSION

Preliminary results were obtained for the reacting fluid flow and heat transfer taking place inside the QQ/LC zones. Due to the twisted mesh, only the r-θ plane plots are given. Figure 6 shows the isotherms and the velocity vectors at the inlet which were taken from the RB zone solutions at the location described in the "description of problem" section. As one can see that, the inlet conditions were nonuniform and with swirl. Accordingly, as done in the previous studies (refs. 3 to 7), assuming uniform, nonswirling inlet conditions to the QQ zone would not be very accurate.

The velocity vectors and isotherms at the center plane of the slot are given in figure 7. Due to the slanted slot, the two vortices, located on both sides of the jet, and the isotherms were not symmetrical about the jet. It can be seen that, near the wall, the high velocity dilution jet deflects the mainstream causing swirl rotating in the direction parallel to the slot. However, near the axis, the mainstream deflects the dilution jet setting up a counter-rotating swirl (in the main flow direction). Figure 8 shows the flow and temperature fields at the end of the slot opening.

The interaction of the inclined jet with the mainstream fluid described above was the cause of the co- and counter-rotating bulk flow pattern shown in figure 9, in which the isotherms are also given. This is the plane located about 1.834 in. downstream of the slot center. From figure 9, there was a high shear layer (HSL) located near the midsection. From the isotherms plot, it can be seen that the HSL mainly contains the lower temperature fluid, an indication of the effect of the jet penetration. The sandwiched-ring-shape (for a whole circle) temperature field, in the order of hot-cold-hot, can be seen clearly in figure 9. This bulk swirl flow and the sandwiched-ring-shape isotherms, typical of the confined slanted jet-in-cross flow, had been observed experimentally (ref. 6).

The bulk swirl flow persisted further downstream as shown in figures 10 and 11. At the end of the divergence section (see fig. 11), the HSL was moving toward the axis due to the increasing flow cross-sectional area At the exit of the LC zone, the bulk swirl flow had almost disappeared and the fluid temperature was in the range of 1250 to 1350 K, as shown in figure 12.

The values of MWSD and PF at various z locations are given in figure 13. The peak shown in the figure was caused by the jet. It was observed from this figure that the fluid was well mixed before leaving the LC zone, indicating that the mixing performance of the STC combustor is very promising. Figure 14 gives the emission index of CO and NO at different z locations. Note that, in this figure, the x-axis represents the distance (in inches) downstream of the fuel nozzle described in part I. Prediction of the NOx emission showed that there was no excessive thermal NOx produced in the QQ/LC zones for the case studied.

To save time in this preliminary study, the calculations were not repeated to match the pressures at the mainstream inlet (or the RB zone pressures at the same location). This coupling study together with parametric studies, such as the STC combustor geometry, momentum flux ratio, mass flow rate redo, slot inclination angle, slot aspect redo, slot number, etc., will be given in the near future.

CONCLUSIONS

In this study, numerical solutions of the chemically reactive flow inside the QQ/LC zones were obtained through a modified version of the KIVA-II code. In the QQ zone, cool dilution air was injected into the hot rich mixture through 45° inclined slot. Results obtained from the RB zone were used as the inlet conditions for the QQ zone. A tension spline interpolation scheme was then used to interpolate the necessary information needed at the mainstream inlet. The jet inlet conditions were chosen closely related to those encountered in advanced combustion systems.

Preliminary results illustrate some of the major features of the flow and temperature fields inside the QQ/LC zones. Formation of the co- and counter-rotating bulk flow and the sandwiched-ring-shape temperature field can be seen clearly and is consistent with experimental observations. From the calculations of the MWSD and the PF of

temperature revealed that the mixing performance of the STC combustor is very good. The temperature of the fluid leaving the LC zone is very uniform. From the results obtained so far, it appears that the modified KIVA-II code can be used to guide the low emission combustion experiments.

ACKNOWLEDGMENTS

REFERENCES

1. S.L. Yang, R. Chen, M.C. Cline, H.L. Nguyen, and G.J. Micklow, "Numerical Simulation of Low Emissions Gas Turbine Combustor Using KIVA-II, Part I:Fuel Nozzle/Rich-Burn Zone Analysis," NASA CR-204141.
2. A.A. Amsden, P.J. O'Rourke, and T.D. Butler, "KIVA-II: A Computer Program for Chemically Reactive Flows with Sprays," Los Alamos National Laboratory Report LA-llS60 MS, May 1989.
3. M.V. Talpallikar, C.E. Smith, and M.C. Lai, "Rapid Mix Concepts for Low Emission Combustors in Gas Turbine Engines," CFD Research Co. Report 4090/1, August 1990.
4. C.E. Smith, M.V. Talpallikar, and J.D. Holdeman, "A CFD Study of Jet Mixing in Reduced Flow Areas for Lower Combustor Emissions," AIAA–91–2460, ALWSAE/ASME/ASEE 27th Joint Propulsion Conference, 1991.
5. M.V. Talpallikar, C.E. Smith, M.C. Lai, and J.D. Holdeman, "CFD Analysis of Jet Mixing in Low NOx Flametube Combustors," ASME Paper 91–GT–217, 36th ASME International Gas Turbine and Aeroengine Conference, 1991.
6. N.S. Winowich, S.A. Moeykens, and H.L. Nguyen, 'Three-Dimensional Calculation of the Mixing of Radial Jets from Slanted Slots with a Reactive Cylindrical Crossflow," AIAA–91–2081, AIAA/SAE/ASME/ASEE 27th Joint Propulsion Conference, 1991
7. G.W. Howe, Z. Li, T. I-P. Shih, and H.L. Nguyen, "Simulation of Mixing in the Quick Quench Region of a Rich Burn-Quick Quench Mix-Lean Burn Combustor," AIAA–91–0410, 29th Aerospace Sciences Meeting, 1991.
8. D.G. Schweikert, "An Interpolation Curve Using A Spline in Tension," J. Math. and Phys., 45, pp. 312–317, 1966.
9. A.K. Cline, "Scalar- and Planar-Valued Curve Fitting Using Splines Under Tension," Comm. of the ACM, 17, pp. 218–220, 1974.
10. S.L. Yang, M.C. Cline, R. Chen, and Y.-L. Chang, "A Three-Dimensional Algebraic Grid Generation Scheme for Gas Turbine Combustors with Inclined Slots," 1992 ASME International Computers in Engineering Conference and Database Symposium, August 2-6, San Francisco, California, Vol. 2, pp. 43–51. Also NASA CR-191095.
11. W.J. Gordon and C.A. Hall, "Construction of Curvilinear Coordinate Systems and Applications to Mesh Generation," Int. J. Num. Meth. Engr., 7, pp. 461–477, 1973.
12. R. Haber and J.F. Abel, "Discrete Transfinite Mappings for the Description end Meshing of Three-Dimensional Surfaces Using Interactive Computer Graphics," Int. J. Num. Meth. Engr., 18, pp. 41–66, 1982.
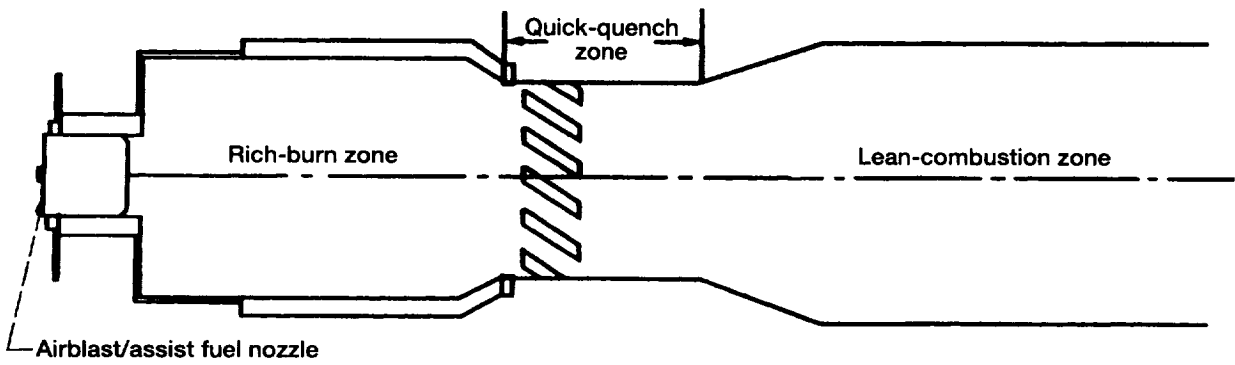
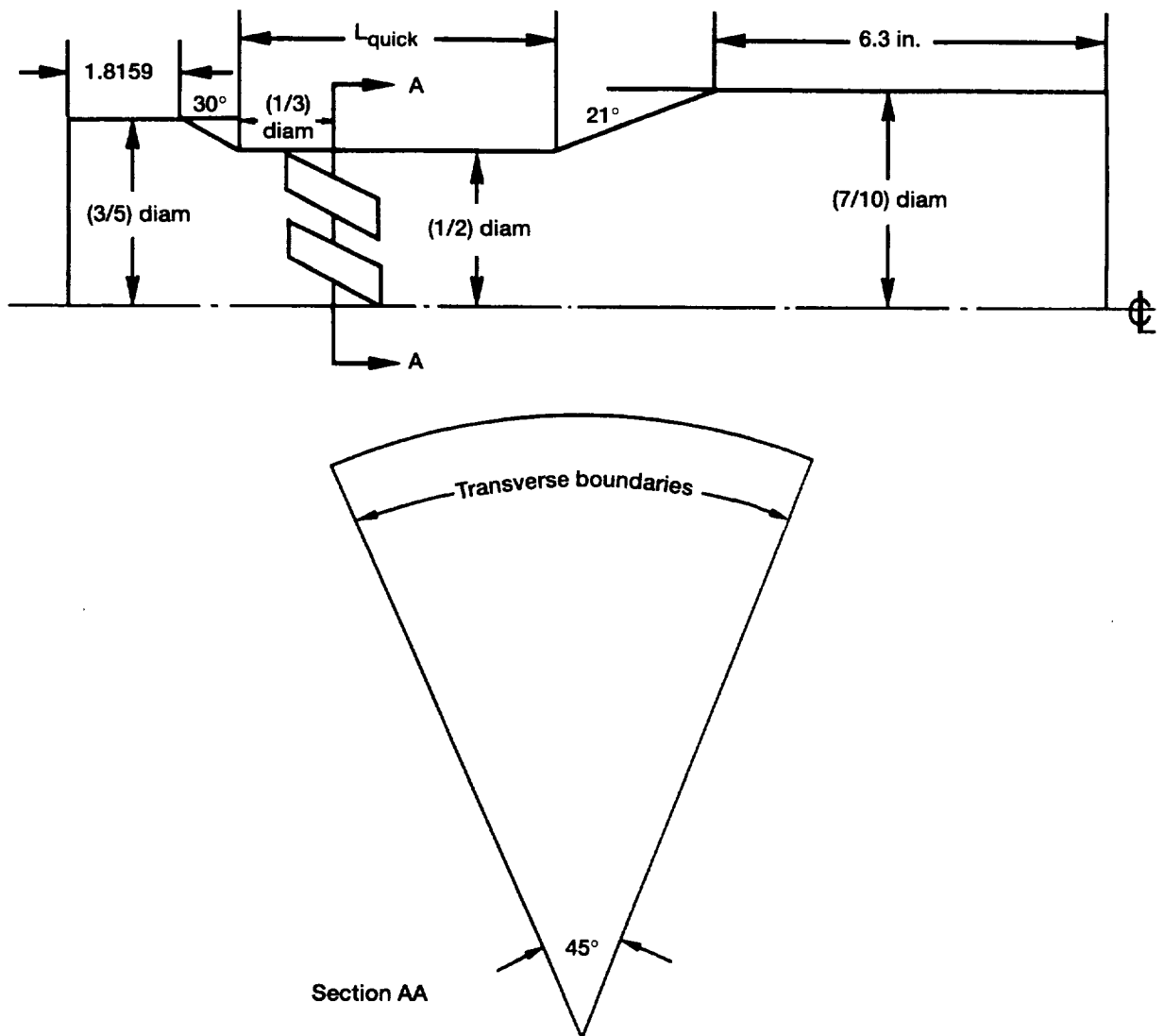Figure 1.—Schematic of a staged turbine combustion.

Section AA

Figure 2.—Geometry of the system under investigation and it's specifications.
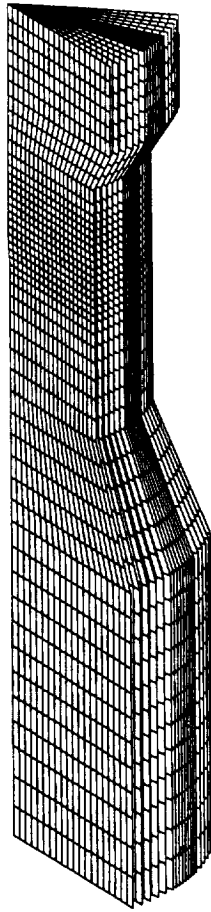
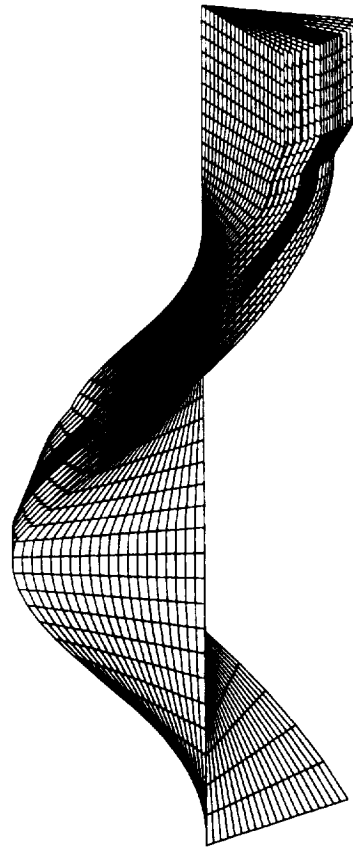Figure 3.—Perspective view of the
grid system before twisting.

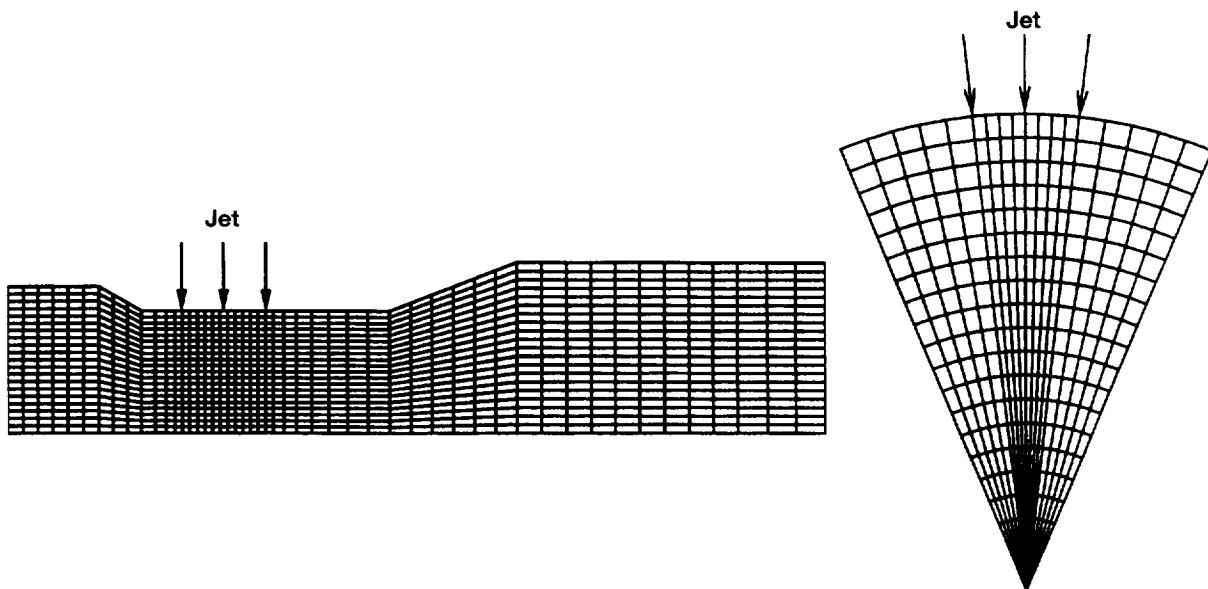Figure 5.—Perspective view of the
grid system after twisting.

Jet

Jet

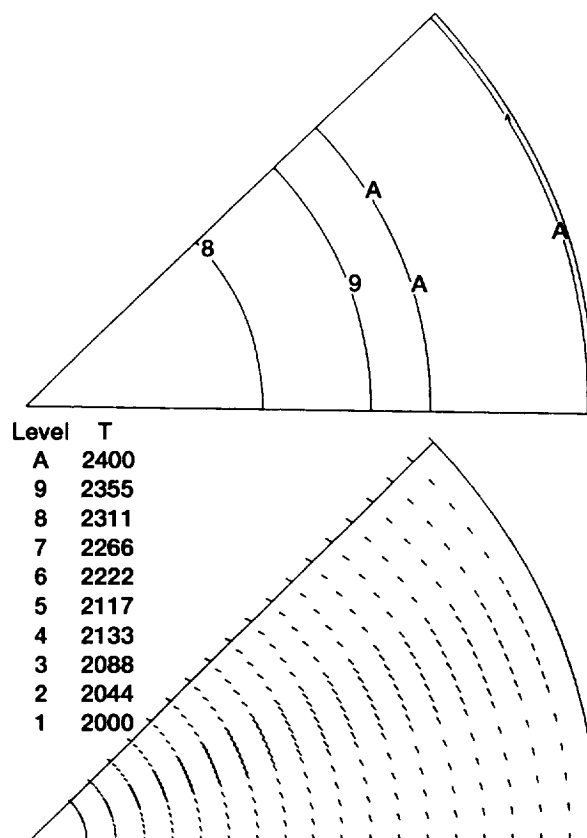Figure 4.—Cross-sectional views of the grid.

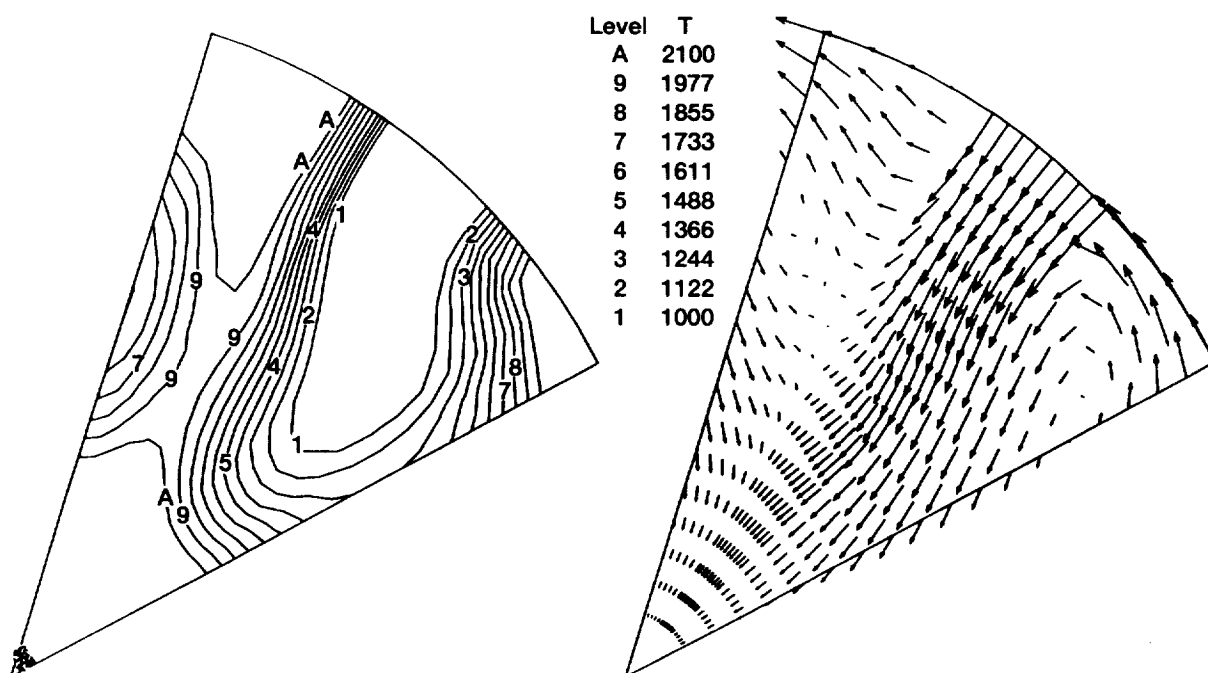Figure 6.—Velocity vectors and isotherms at the inlet.

Level	T
A	2400
9	2355
8	2311
7	2266
6	2222
5	2117
4	2133
3	2088
2	2044
1	2000

Figure 7.—Velocity vectors and isotherms at the center plane of the slot.

Level	T
A	2100
9	1977
8	1855
7	1733
6	1611
5	1488
4	1366
3	1244
2	1122
1	1000

Level	T
A	1900
9	1800
8	1700
7	1600
6	1500
5	1400
4	1300
3	1200
2	1100
1	1000
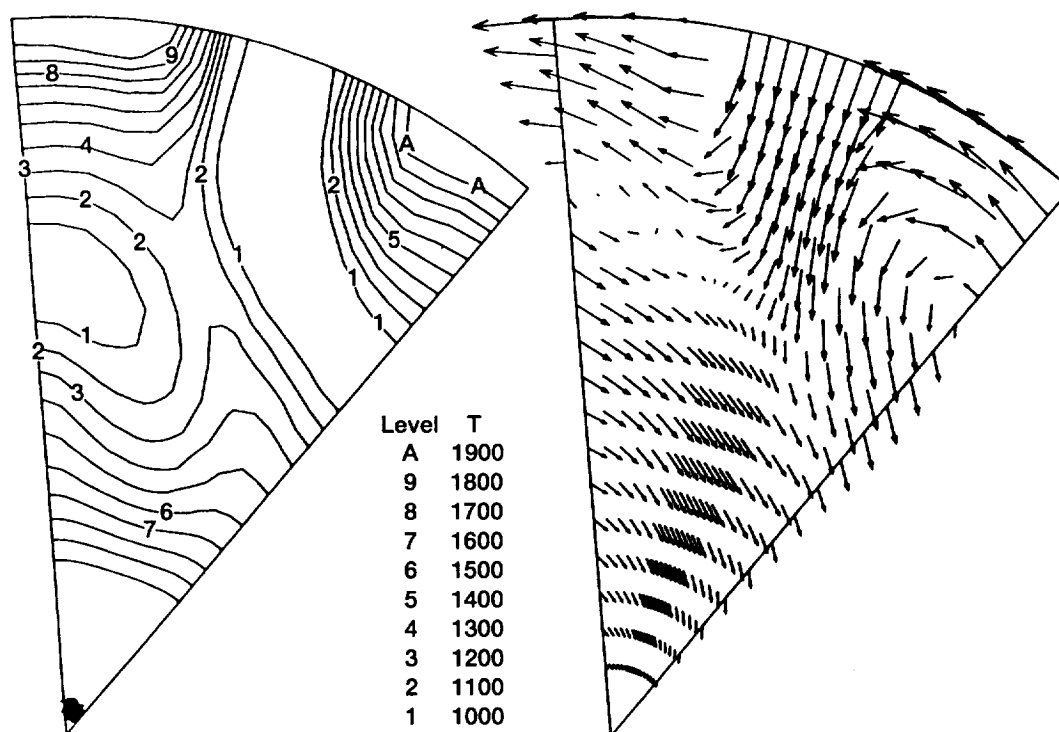
Figure 8.—Velocity vectors and isotherms at the end plane of the slot.

Level	T
A	1900
9	1822
8	1744
7	1666
6	1588
5	1511
4	1433
3	1355
2	1277
1	1200
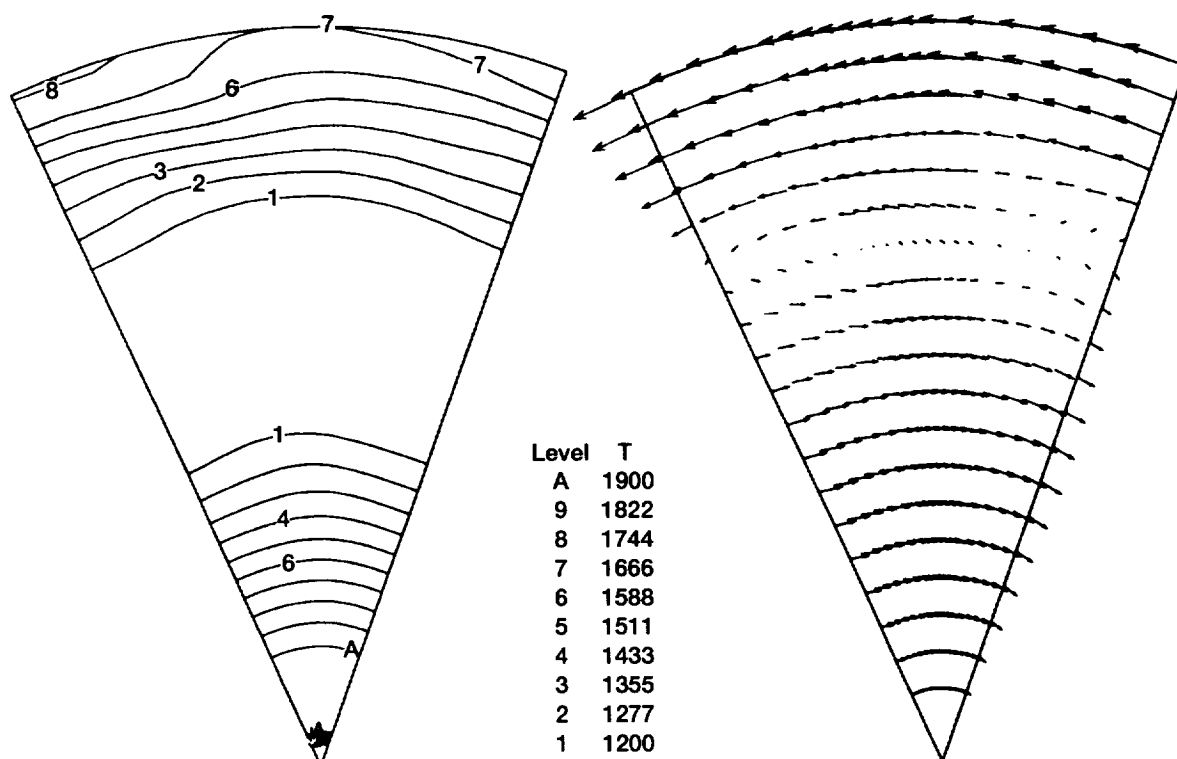
Figure 9.—Velocity vectors and isotherms at the 1.834 in. downstream of the slot center plane.

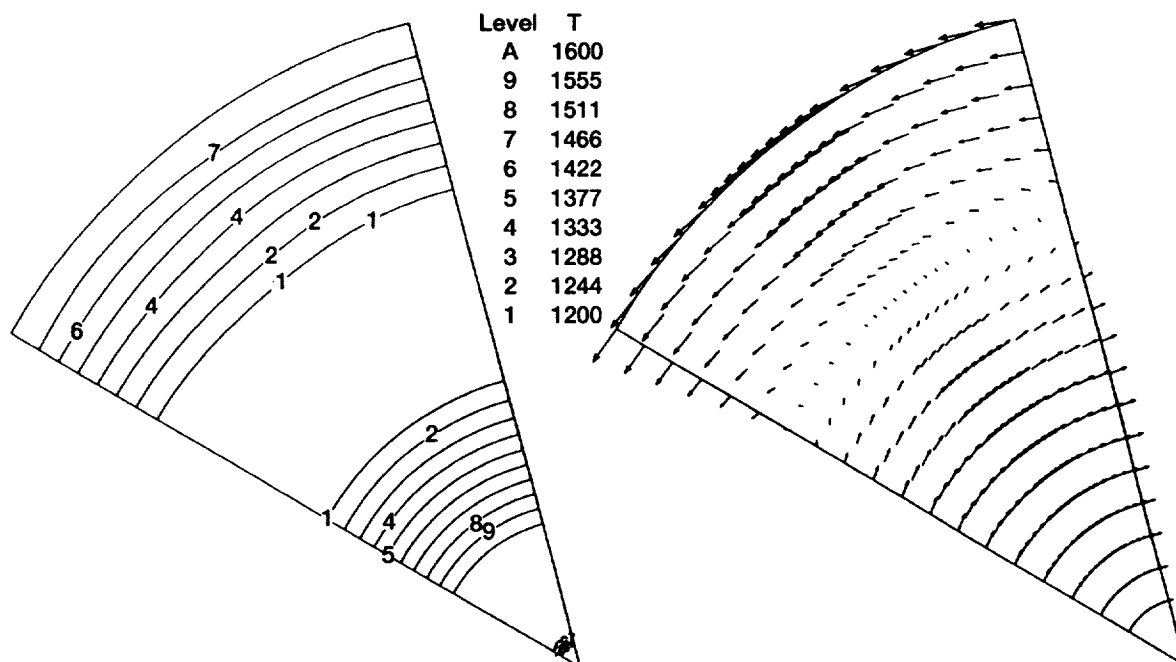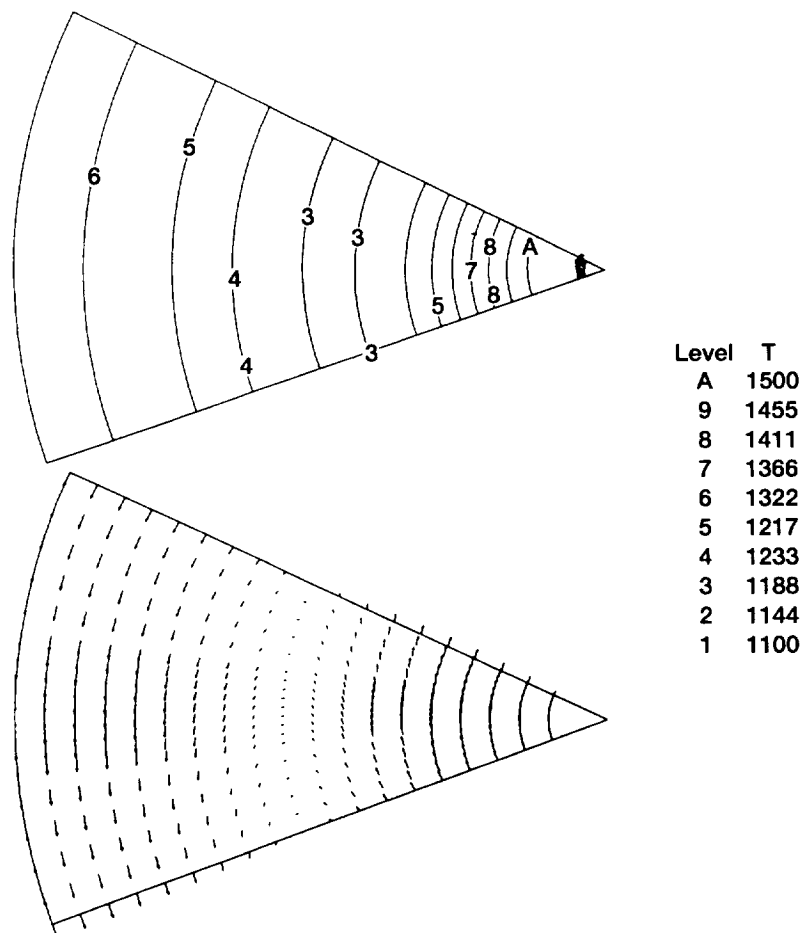| Level	T
A	1600
9	1555
8	1511
7	1466
6	1422
5	1377
4	1333
3	1288
2	1244
1	1200

Figure 10.—Velocity vectors and isotherms at the beginning of the divergence section.

Figure 11.—Velocity vectors and isotherms at the end of the divergence section.
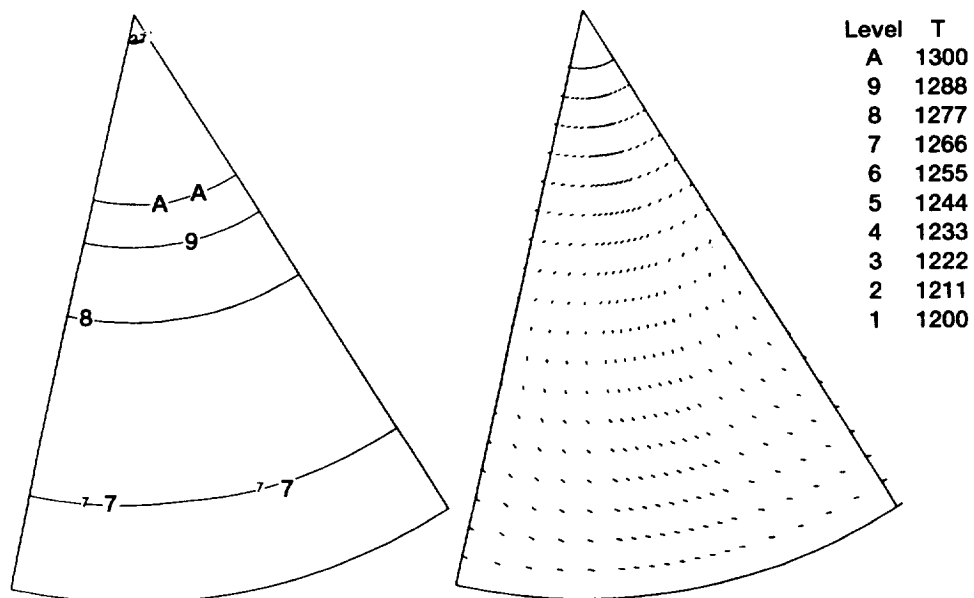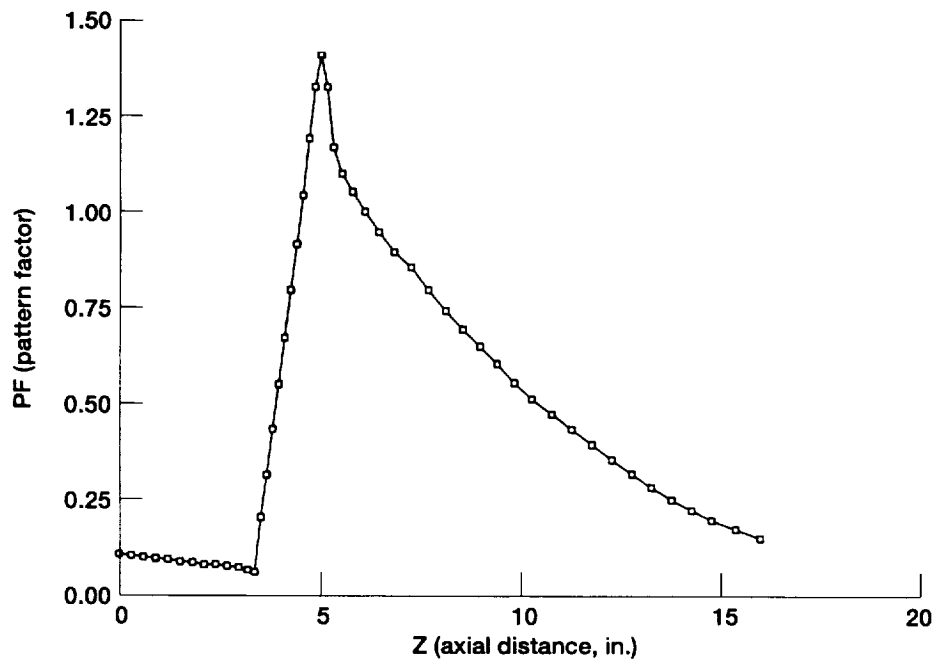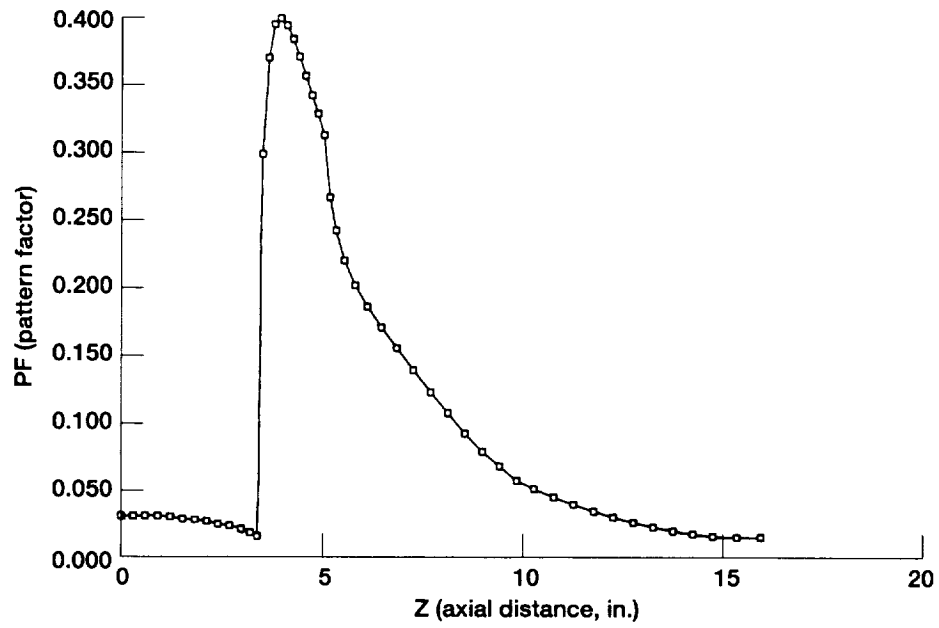
Level	T
A	1500
9	1455
8	1411
7	1366
6	1322
5	1217
4	1233
3	1188
2	1144
1	1100

Level	T
A	1300
9	1288
8	1277
7	1266
6	1255
5	1244
4	1233
3	1222
2	1211
1	1200

Figure 12.—Velocity vectors and isotherms at the outler plane.

Figure 13.—MWSD and PF.

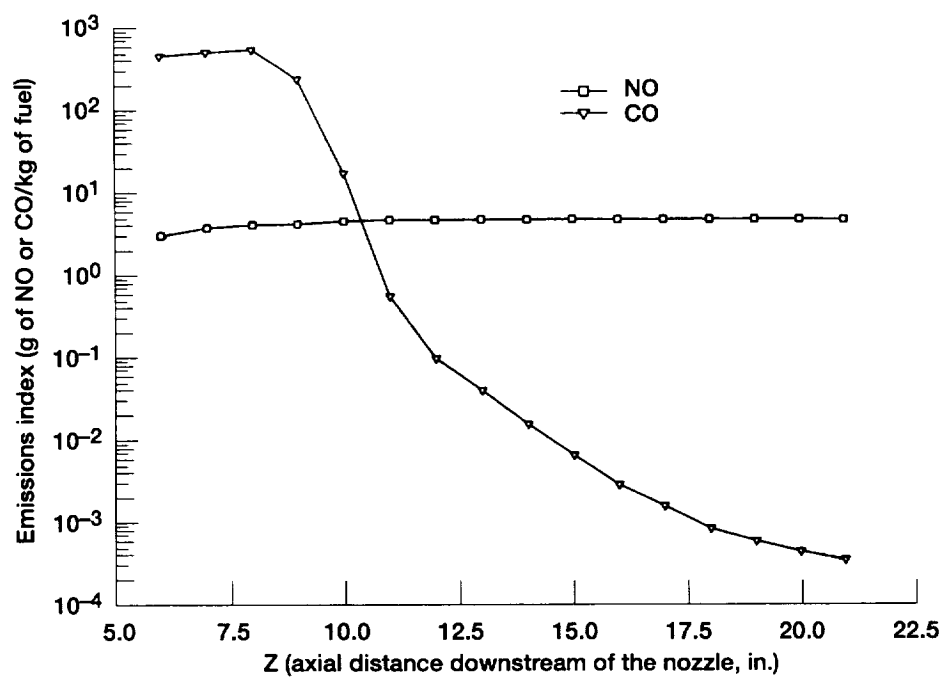Figure 14.—Emission index of CO and NO.

REPORT DOCUMENTATION PAGE

Public reporting burden for this collection of information is estimated to average 1 hour per response, including the time for reviewing instructions, searching existing data sources, gathering and maintaining the data needed, and completing and reviewing the collection of information. Send comments regarding this burden estimate or any other aspect of this collection of information, including suggestions for reducing this burden, to Washington Headquarters Services, Directorate for Information Operations and Reports, 1215 Jefferson Davis Highway, Suite 1204, Arlington, VA 22202-4302, and to the Office of Management and Budget, Paperwork Reduction Project (0704-0188), Washington, DC 20503.

1. AGENCY USE ONLY (Leave blank)	2. REPORT DATE August 1996	3. REPORT TYPE AND DATES COVERED Final Contractor Report

4. TITLE AND SUBTITLE

Numerical Simulation of a Low Emissions Gas Turbine Combustor Using KIVA-II

Part II: Quick-Quench/Lean-Combustion Zones Analysis

6. AUTHOR(S)

S.L. Yang, R. Chen, and M.C. Cline

5. FUNDING NUMBERS

WU–523–26–33–00

G–NAG3–1109

7. PERFORMING ORGANIZATION NAME(S) AND ADDRESS(ES)

Michigan Technological University
ME-EM Department
Houghton, Michigan 49931

8. PERFORMING ORGANIZATION REPORT NUMBER

E–7213

9. SPONSORING/MONITORING AGENCY NAME(S) AND ADDRESS(ES)

National Aeronautics and Space Administration
Lewis Research Center
Cleveland, Ohio 44135–3191

10. SPONSORING/MONITORING AGENCY REPORT NUMBER

NASA CR–204140

11. SUPPLEMENTARY NOTES

12a. DISTRIBUTION/AVAILABILITY STATEMENT

Unclassified - Unlimited
Subject Categories 34 and 05

This publication is available from the NASA Center for AeroSpace Information, (301) 621–0390.

12b. DISTRIBUTION CODE

13. ABSTRACT (Maximum 200 words)

This is the second part of the numerical investigation on a low emissions staged turbine combustor (STC) using a modified version of the KIVA-II code. The main focus of this study is the numerical analysis of the reacting fluid flow and heat transfer inside the quick-quench/lean-combustion (QQ/LC) zones. In the QQ zone, cool dilution air was injected into the hot mixture through eight 45° inclined slots with a momentum flux ratio of 60. The slot aspect ratio was 6 and the jet-to-mainstream mass flow rate ratio was 3. The inlet conditions of the QQ zone were obtained from the results of rich combustion zone analysis described in part I. A tension spline interpolation scheme was then used to interpolate the necessary information needed at the inlet. Conditions at the slot opening (dilution jet) were chosen closely related to those encountered in advanced combustion systems. The Grid system needed for the numerical solutions was generated by a transfinite interpolation scheme. KIVA-II was further modified for the current study. Preliminary results illustrate some of the major features of the flow and temperature fields inside the QQ/LC zones. Formation of the co- and counter-rotating bulk flow and the sandwiched-ring-shape temperature field, typical of the confined inclined jet-in-cross flow, can be seen clearly and is consistent with experimental observations. The calculations of the mass-weighted standard deviation and the pattern factor of temperature revealed that the mixing performance of the STC combustor is very promising. The temperature of the fluid leaving the LC zone is very uniform. Prediction of the NOx emission index showed that there was no excessive thermal NOx produced in the QQ/LC zones for the case studied. From the results obtained so far, it appears that the modified KIVA-R code can be used to guide the low emission combustion experiments.

14. SUBJECT TERMS

Gas turbine combustors; CFD; Emissions; Dilution jet mixing

15. NUMBER OF PAGES 15

16. PRICE CODE A03

17. SECURITY CLASSIFICATION OF REPORT	18. SECURITY CLASSIFICATION OF THIS PAGE	19. SECURITY CLASSIFICATION OF ABSTRACT	20. LIMITATION OF ABSTRACT
Unclassified	Unclassified	Unclassified	